Hindawi
Geofluids
Volume 2022, Article ID 9355020, 10 pages
https://doi.org/10.1155/2022/9355020

*Research Article*

# Study on Pore Structure of Shale Reservoir by Low Temperature Nitrogen Adsorption Method

**Huaying Mi**,[1] **Yujie Guo**,[2] **and Xiaogang Yu**[3]

[1]*School of Electronics and Internet of Things Engineering, Chongqing Industry Polytechnic College, Chongqing 401120, China*
[2]*Gas Production Plant 5 of PetroChina Changqing Oilfield Company, CNPC, Ordos 017300, China*
[3]*Exploration and Development Research Institute of Huabei Oilfield, Renqiu 062552, China*

Correspondence should be addressed to Huaying Mi; mihy@cqipc.edu.cn

Received 29 March 2022; Revised 24 May 2022; Accepted 1 June 2022; Published 21 June 2022

Academic Editor: Dengke Liu



Shale gas is one of the most actively explored unconventional sources of natural gas. There are several types of pores in the shale reservoir, and their structural characteristics are complex. Evaluating the characteristics of the shale pore structure is the basis for understanding the shale reservoir performance and the oil and gas migration mechanism. In this paper, the micro- and nanopores of shale samples from the Yanchang Formation, Hunan basin, are studied by applying the low-temperature nitrogen adsorption method. Several pore structure parameters such as the specific surface area, the pore volume, and the pore size distribution of the analyzed samples are calculated. The predominant characteristics of nanopores that influence hydrocarbon accumulation and control the development of pores are discussed. The results indicate that the shale reservoir rocks from the study area are mainly mesoporous with an average pore size distribution between 2 and 50 nm. A small number of micropores (less than 2 nm) and macropores (more than 50 nm) are also present in the pore network. The development of micropores and mesopores in the shale samples is associated with organic matter content, while the development of macropores is linked to clay minerals content. Total organic carbon (TOC) content is the key element to control the nanopore volume and the specific surface area of the reservoir rocks from the study area. At the same time, the organic matter-enriched pore network also provides extensive space for the accumulation of shale gas.

## 1. Introduction

Due to advances in technology, global energy consumption continues to grow, while people's dependency on oil and gas increases. In recent years, unconventional energy, including shale gas, has attracted widespread attention from researchers, as well as petroleum companies. The exploration and development of shale gas provide a distinct approach to solving the global energy shortage. In terms of shale gas exploration, exploitation, and development, the Sichuan-Chongqing-Guizhou provinces have been the main research region in China during the past ten years, fully demonstrating the broad prospects of Paleozoic shale gas in the southern part of China. Compared to conventional resources, shale gas is characterized by generation and storage in the source rock. The formation plays the role of source rock and a reservoir but also that of a caprock. Shale gas mainly exists in an adsorbed and a free state, and its state of occurrence depends on the pore-throat size of the rock, indicating different phase states in pores of different types and sizes. While the exploration and development of shale oil and gas have become a topic of interest, many researchers have demonstrated that the nanoscale pore structure characteristics of the reservoir have an important impact on the exploration and development of shale oil and gas [1–3].

At the same time, a clear and precise understanding of the pore structure characteristics in shale oil and gas reservoirs does not only give experimental support for optimizing the horizon of sweet spots and evaluating the classification of reservoirs but also provides a basis for further research on the occurrence and seepage mechanism of shale oil and gas. The fluid intrusion method examines the connected pores in the sample by injecting fluid into the sample, which includes high pressure mercury porosimetry (MICP) [4],

adsorption method [5], and He-specific gravity method. The main principle of the fluid intrusion method is to inject nonwetting fluid and various gases into the sample and record the corresponding injected amount under different pressure values. The most used fluid intrusion methods are high pressure mercury porosimetry (MICP) and gas adsorption. Additional information on parameters such as porosity, specific surface area, and pore size distribution can also be obtained if the experimental data of the fluid intrusion method is combined with different theoretical methods. Sisk et al. used digital petrophysical techniques to study the porosity of shale reservoirs in North America and concluded that the shale pore sizes are mainly distributed in the range between 3 and 15 nm. Ambrose et al. studied the pore structure characteristics of shale by using the high-pressure mercury injection method and established the conversion relationship between the capillary pressure PC and the reservoir parameters. Lin Xiaoying et al. analyzed and studied the effects of soluble organic matter on shale pore structure based on laboratory core testing methods.

Currently, under laboratory conditions, the physical test method is mainly used to analyze the rock microstructure of the shale reservoir. Most of these methods are based on conclusions from the experimental techniques performed on conventional reservoirs and coal seams. There are several different types of micro- and nanopores in shale reservoir rocks. Additionally, there are numerous mineralogical components. The complex pore space structure and the diagenetic environment pose new challenges to the conventional test methods. They cannot effectively characterize the microstructure and the morphological characteristics of shale reservoir rocks. The cast thin section method can identify the pore distribution and the morphological characteristics in the rock sample by injecting colored glue into the rock pores. However, since it is required to wash and pour the core sample during the preparation process, identification of the pore throat may be affected. Moreover, due to the limited resolution of the polarizer, it cannot adequately determine the micropores in the rock core.

Scanning electron microscopy (SEM) can detect micro- and nanopores developed in rock samples by triggering the incident beam of electrons and is used for the analysis of core surface features. Its main advantage is that it can directly observe the real characteristics of pores and then converts the image into quantitative data such as pore size distribution and porosity. Currently, domestic and foreign scholars have used the focused ion beam-helium ion microscopy (FIB-HIM) technique to analyze the particularities of organic matter derived pores in shale core samples [6] and the scanning electron microscopy (SEM) technique to qualitatively describe and to quantitatively characterize the microscopic pore structure of shales [7–9]. However, during the actual operation process, the image analysis method has several deficiencies. For example, nonexistent pores may be generated during the sample pretreatment process [10], and the image method cannot distinguish the false pores from the real pores [11]. At the same time, microscopic analyses often lack representativeness and cannot fully display the structural characteristics of the samples. It is difficult to accurately reflect the complex pore characteristics in the rock sample because the magnification of the high-resolution backscatter image method has some limitations; however, the pore morphology of the image can be observed. In addition to the previously mentioned shortcomings, several factors can affect the accuracy and reliability of the imaging studies, such as the characteristics of the sample itself, the used method for sample preprocessing, and the performance of the resolution instrument [12]. Although electron microscopy performs high resolution images and allows nanoscopic scale observations, it is still unable to achieve a full-scale quantitative description of pores. Therefore, its practical applications are limited.

The high-pressure mercury intrusion method (MICP) primarily measures connected macropores with pore sizes greater than 100 nm. This method has a simple structure and can adequately characterize the pore network of diagenetic and conventional reservoir rocks. However, the high-pressure mercury intrusion method can only detect some mesopores and macropores which cannot be analyzed, due to the large pore size range of shale oil and gas reservoirs, the complex pore network of shales, the variety of pore shapes, and the development of micropores. The majority of the pores will severely affect the mercury saturation during the mercury intrusion process, resulting in deviations of the test results. Additionally, the injection pressure required for the mercury solution to enter the macropores is relatively low and does not affect the reservoir samples, while the injection pressure required to inject the mercury solution into the mesopores and the micropores is relatively high and can easily damage the shale reservoirs. Since there is a significant amount of large micro-nanopores in the shale layers which generate cracks, the accuracy of the measurements is affected. The low-temperature gas adsorption method can efficiently detect the micropores in the experimental samples by selecting the gas of appropriate particle sizes as the adsorbent. There is a study of the porosity characteristics of underground rocks.

The low-temperature nitrogen adsorption method primarily measures the connected mesopores with pore sizes varying between 1.2 and 200 nm. Its hysteresis loop can be examined through the nitrogen adsorption-desorption isotherm, thereby attaining the description of the pore network. The size, shape, and network type of shale pores can be determined by analyzing the nitrogen adsorption-desorption isotherms and the hysteresis loop types. Furthermore, the obtained images can be used to distinguish the kerogen type and examine the development of the organic pores. Both international and domestic scholars have carried out numerous studies using the low-temperature nitrogen adsorption technique. Han et al. compared the effects of the sample particle sizes and water contents on nitrogen adsorption [13]. Zapata et al. and Yang et al. obtained nitrogen adsorption isotherms by studying nitrogen adsorption isotherms. The influence of the properties of adsorbents and adsorbates was discussed [14, 15]. Keluo et al. described the relationship between the surface area, the pore volume, and the pore type by analyzing the nitrogen adsorption capacity [16].

## 2. Sampling and Methodology

*2.1. Sampling.* According to the field outcrop sampling data and the measured geological profile, the distribution of the shale reservoir rocks from the Yanchang Formation can describe the characteristics of the shale gas reservoir in the study area. This perimeter belongs to the inland Hunan sedimentation and is characterized by several microfacies such as lake bottom fan, lakeside sand bar, and argillaceous lake beach. The predominant lithology is represented by alternating thin gray siltstone layers and dark gray to black shale layers. The sandstone contents are minor. The deposition of the productive interval is characterized by strong cyclicity. During the actual exploration and development processes, the formation is further divided into ten subdivisions based on typical marker beds. The samples used in our study were collected from the dark shale located at the bottom of the productive interval. Numerous layers of dark shale developed in the productive interval are rich in organic matter and clay minerals. The total organic carbon content (TOC) varies between 0.18% and 6.60%, with an average value of 3.96%.

*2.2. Analytical Methods.* Before performing the experiments, the samples were collected, crushed, and screened according to national standards. The mineralogical composition of the samples was determined by using a D8 discover X-ray diffractometer.

The low-temperature nitrogen adsorption method of the shale reservoir rock samples was performed by using an ASAP2020 instrument developed by Micrometrics (Figures 1–3), which can efficiently measure the pore size distribution of the analyzed rock samples. The nitrogen adsorption instrument can study the distribution of pores with diameters in the size range of 0.35–500 nm, in which the effective detection limit of the microporous section is 0.02 nm, the controllable range of the relative pressure (P/P0) during the experiment is 0.001-0.998, the lower limit of detection of the shale pore specific surface area is 0.0005 $m^2$/g, and the minimum resolution of the pore volume is 0.0001 $cm^3$/g.

*2.3. The Nitrogen Adsorption Method.* Initially, it is necessary to remove the impurities from the samples and then put the samples in the liquid nitrogen environment. Afterwards, the amount of nitrogen adsorbed by the rock sample under the corresponding state is measured by regulating the external gas pressure, and subsequently, the adsorption-desorption isothermal curve is obtained [17]. The geometric shape of the pores can be determined by the adsorption-desorption return line, and the corresponding empirical model can efficiently calculate the typical parameters such as pore size, pore volume, and specific surface area [18–20].

Before performing the experiment, to remove the impurities, all samples are fully degassed under high-temperature conditions and vacuumed for a fixed period. Afterwards, the samples are put into a Dewar bottle that contains liquid nitrogen connected to the instrument analysis system. The volumetric method is used to determine the measured rock sample in a high-purity liquid nitrogen environment, with an experimental controlled temperature at 77.4 K. The absorption of the adsorbate substance by the analyzed rock sample can be efficiently measured by adjusting the experimental gas pressure at a certain period. Finally, the curve of gas absorption versus relative pressure is obtained, which represents the low-temperature nitrogen adsorption loop.

The traditional adsorption theory does not clarify the adsorption mechanism. On these terms, Brunauer et al. proposed the multimolecular adsorption BET model. In the BET model, the specific surface areas of the samples are obtained by applying the linear regression model. By calculating the saturated adsorption capacity of the monolayer in the analyzed samples, the corresponding BET specific surface area can be obtained. The pore diameter is calculated by applying the Kelvin method. For most mesopores, the BJH (Barret Joyner Halenda) model in association with the Kelvin and the Halsey equations is used to determine the pore diameter distribution. For the micropores which are formed by the special structure of clay crystal layers in shales, the DA (Dubinin Astakhov) principle can be applied for performing the corresponding calculations. The experimental pressure can reach the gas pressure by adjusting the experimental temperature and by controlling the experimental pressure. Consequently, the pore volume and the average pore diameter can be efficiently characterized by calculating the gas adsorption capacity of the measured sample.

Because there are several types of pores in the shale reservoir that are defined by complex structural characteristics, domestic research regarding the internal reservoir porosity of shale reservoirs is lacking theoretical support. Some commonly used laboratory core detection techniques have not established a systematic methodology regarding shale reservoir porosity in view of conventional reservoirs and coal seams [21–23]. Generally, researchers refer to the IUPAC (International Union of Pure and Applied Chemistry) as the widely used standard in the fossil energy industry for the classification of the reservoir rock pore space: micro (small) pores (pore size < 2 nm), mesoporous (mesoporous) (2 nm < pore size < 50 nm), and macro (large) pores (pore size > 50 nm). The phenomenon of desorption lag often occurs when measuring the adsorption isotherm of porous media. Typically, in the low-temperature nitrogen adsorption method, the adsorption curve and the desorption curve gradually separate with the increase of the relative gas pressure. Consequently, an adsorption-desorption return line is formed in the high-pressure area, which is usually accompanied by capillary condensation. As expected, by adjusting the experimental pressure, capillary condensation will occur in the pore network of the analyzed samples. By continuously increasing the experimental pressure, the lower limit of the capillary condensation will also increase. When the relative gas pressure values are invariable, the development of capillary condensation in the reservoir rock pores depends on the critical pore radius rk [21, 22, 24]. Specifically, the capillary condensation that can cause the adsorbent to fill smoothly only occurs in the pore spaces where the rock pore sizes are less than rk, and the adsorbent cannot enter in the pore spaces where the pore sizes are greater than this maximum value.


Figure 1: ASAP2020 instrument developed by Micrometrics.

Figure 2: The analyzed drill core samples.


Figure 3: Calculation of the rock sample porosity distribution.

Table 1: Fundamental analysis data of shale samples.

| Sample no. | TOC (%) | Quantitative analysis of whole rock (%) | | | | | | | Clay minerals |
|---|---|---|---|---|---|---|---|---|---|
| | | Quartz | Potassium feldspar | Plagioclase | Calcite | Dolomite | Pyrite | Siderite | |
| L-2 | 1.66 | 34 | 5 | 39 | 0 | 2 | 0 | 0 | 20 |
| L-3 | 2.67 | 30 | 7 | 15 | 3 | 10 | 0 | 5 | 30 |
| L-5 | 4.49 | 37 | 6 | 25 | 0 | 0 | 0 | 3 | 29 |
| L-6 | 3.19 | 39 | 7 | 24 | 2 | 0 | 0 | 0 | 28 |
| L-21 | 0.68 | 32 | 4 | 15 | 1 | 0 | 0 | 7 | 41 |
| L-24 | 6.60 | 21 | 2 | 11 | 29 | 5 | 0 | 9 | 23 |
| L-27 | 5.26 | 23 | 7 | 26 | 0 | 0 | 1 | 4 | 39 |
| L-29 | 5.65 | 29 | 6 | 11 | | 4 | | | 50 |
| L-35 | 6.53 | 24 | 2 | 22 | 0 | 13 | 0 | 0 | 39 |

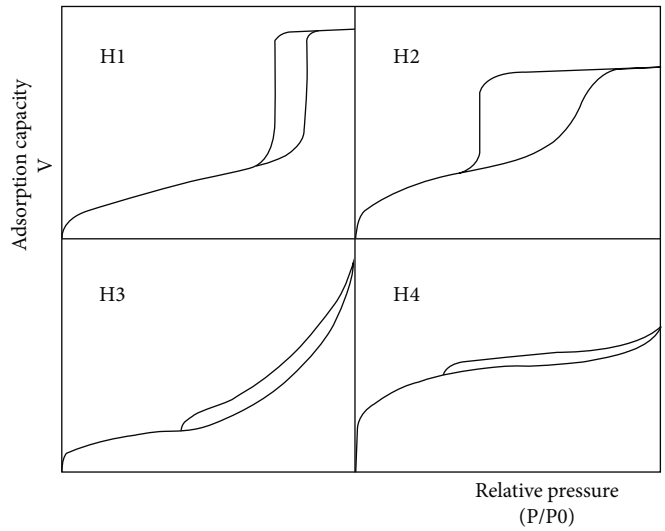


Figure 4: Hysteresis loops recommended by the International Union of Pure and Applied Chemistry.

There are several adsorption mechanisms in rocks with pores of different sizes. Nitrogen is mostly adsorbed and filled by a single gas molecule in the micropores of the reservoir rocks. In mesopores, there are various states. When the relative pressure is low, the gas adsorption state is similar to the one in micropores. With the continuous increase of the relative pressure, it gradually shifts to the superposition adsorption of multiple gas molecules. In particular, when the gas pressure is high, condensate will start accumulating in the pores. When the relative pressure is low, the adsorption state of gas molecules in macropores is similar to the one in mesopores. However, with the increase of the gas pressure, capillary condensate will accumulate in such pores.

Table 2: Pore structure parameters of the shale samples.

| Rock specimen | Parameter | | |
|---|---|---|---|
| | Specific surface area ($m^2/g$) | Pore volume (mL/g) | Average aperture (nm) |
| L-2 | 3.098 | 0.55145 | 7.912 |
| L-3 | 3.055 | 0.12405 | 11.015 |
| L-5 | 4.245 | 0.07801 | 6.813 |
| L-6 | 12.942 | 0.35335 | 4.689 |
| L-21 | 7.684 | 0.14541 | 5.89 |
| L-24 | 3.484 | 0.13379 | 7.689 |
| L-27 | 3.078 | 0.36145 | 8.214 |
| L-29 | 3.684 | 0.20705 | 7.215 |
| L-35 | 2.968 | 0.17465 | 9.925 |

## 3. Results and Discussion

*3.1. Mineralogical Composition.* The mineralogical composition of the analyzed samples is listed in Table 1. The shale reservoir samples are characterized by varying concentrations of potassium feldspar, plagioclase, dolomite, siderite, and other minerals. The composition is relatively complex, and the predominant minerals are represented by quartz and clay minerals, with contents up to 50%. The complex structure between the clay crystal layers allows the development of indispensable micropores in the shale samples. The emergence of numerous micropores does not only expand the pore space in the reservoir rocks but also provides a larger capacity for the adsorption of hydrocarbons.

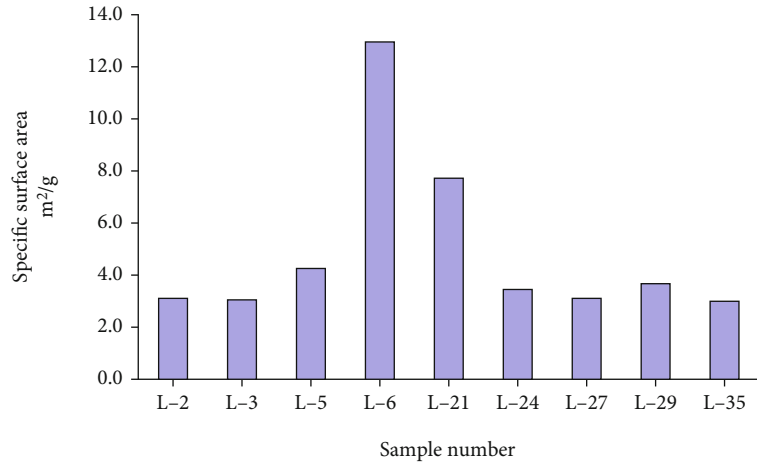


Figure 5: Stratigraphical distribution of the surface area of the shale samples.

*3.2. Adsorption Isotherm.* Different types of pores generate distinct patterns of adsorption-desorption loops, which means that the pore characteristics can be efficiently determined based on the specific loop patterns. According to the characteristics of the adsorption-desorption return line initially described by de Boer, the International Union of Pure Chemistry and Applied Chemistry (IUPAC) classifies the adsorption-desorption return lines obtained from low-temperature gas adsorption methods into four typical categories, as illustrated in Figure 4.

In Figure 1, the H1 and H4 loops outline two extreme forms, while the H2 and H3 loops represent the intermediate form. When the relative pressure reaches a certain value, the adsorption and desorption curve of H1 quickly changes with a continuous increase, indicating that the gas adsorption capacity is strongly influenced by changes in the relative pressure. However, when the relative pressure reaches a certain value, as it continues to increase, the adsorption and desorption curve in H4 slowly changes. This means that changes in the relative pressure do not influence the gas adsorption capacity. By analyzing the shape of the adsorption-desorption return line measured during the analytical phase, the characteristics of the porosity in rock samples can be determined. The H1 loop is observed in porous media and spherical aggregates with a uniform particle size distribution. The H2 type loop can be recognized in the gel and the wide diameter block. The H3 loop can be identified in clayey and silty environments accumulated by particle adsorption. Generally, this kind of environment has no upper limits of adsorption, which means that there is no saturated adsorption state. The H4 hysteresis loop can be observed in the porous active environment in association with pore gap development. This type of loop is characterized by the absence of a saturated adsorption phenomenon and indicates that a certain amount of micropores are formed in the environment.

Although there are minor morphological differences between the analyzed rock samples, the corresponding adsorption and desorption curves indicate an anti "*s*" shape. With the gradual increase of the experimental relative pressure, the front section of the adsorption curve rises slowly with a slightly upward direction. Additionally, the adsorption curve suddenly becomes steeper. Particularly, when the experimental pressure is extremely close to the gas pressure, then there is an absence of the horizontal line, which suggests saturation. From the perspective of the adsorption mechanism, there is evidence that capillary condensation occurs in the pores of the reservoir rocks. Specifically, the first half of the adsorption line slowly rises and protrudes slightly upward in the section with low relative pressure ($0 < P/P0 < 0.1$, P0 is the saturated gas pressure in the experimental state). At the same time, liquid nitrogen adsorbs a single gas molecule on the shale surface, gradually fills the micropores in the rock, and transitions to the multimolecular layer. In the middle section of the adsorption line, when the pressure rises to a certain range ($0.1 < P/P0 < 0.4$), the gas pressure has an almost linear correlation with the gas adsorption capacity. This indicates that the adsorbed gas is adsorbed on the rock surface of the shale reservoir. With the continuous increase of the relative pressure, the adsorption curve of the rock sample gradually rises and displays a downward concave shape. During the period of high relative pressure ($P/P0 > 0.4$), the measured adsorption curve of the rock sample rises sharply until the experimental gas pressure $P$ approaches the saturated steam pressure P0. Therefore, when the relative pressure $P/P0$ is approximately 1, then there is no adsorption saturation. This indicates that a certain number of mesopores and macropores are developed in the rock samples of the shale reservoir. The adsorption mechanism during this stage is primarily manifested in the capillary condensation of the rock samples, which makes the adsorbent enriched in its pore space. At the same time, the adsorption line and the desorption line of the rock sample do not coincide, consequently forming a hysteresis loop.

By analyzing and studying the shape of the adsorption-desorption return lines measured during the experimental phase, the pore space characteristics of the rock samples can be efficiently determined. According to the IUPAC classification standards, the adsorption-desorption return lines of the four shale samples are similar to the H3 type and have the morphological characteristics of the H4 type, which combines the characteristics of the two types of curves. This

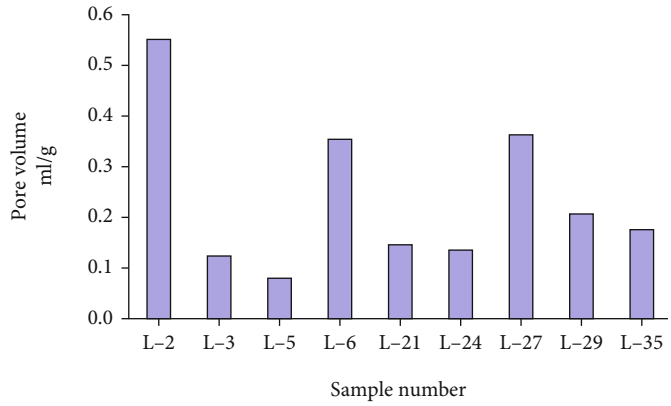


Figure 6: Stratigraphical distribution of the pore volume.

also indicates that micro- and nanosized pores are developed in the shale reservoir rocks from the study area, and that there is no fixed geometric shape. The internal pores of the rock samples are mainly flat and mixed with multiple types of amorphous pores. At the same time, the lag ring of the rock samples is small. Compared to the H3 standard loop, it can be inferred that many pores with different sizes are developed in the rock sample, and the pore spaces with a well-connected network are more conducive to the storage and migration of hydrocarbons in shales.

*3.3. Specific Surface Area of the Shales.* The gas adsorption capacity corresponding to the infinite approximation of the experimental pressure in the adsorption loop to the saturated pressure is considered as the pore volume of the measured rock sample. In this case, the classical BET model formula is selected to calculate the specific surface area of the rock samples. The pore structure parameters of the shale reservoir samples from the study area are shown in Table 2 and Figures 5 and 6.

It can be observed from Figures 2 and 3 that the rock sample L-6 is characterized by the most outstanding pore network development (the balance between pore volume and pore specific surface area). The specific surface area is 12.942 $m^2$/g, and the pore volume is 0.35335 mL/g. The pore network development of the rock samples L-3 and L-35 is relatively poor, the specific surface areas are 3.055 $m^2$/g and 2.968 $m^2$/g, respectively, while the pore volumes are 0.12405 mL/g and 0.17465 mL/g, respectively. The average value of the specific surface area of the samples is 4.915 $m^2$/g, and the average pore volume value is 0.23658 mL/g.

*3.4. Implication of Shale Porosity for Gas Storage.* The significance of shale pore volume (pore surface area) for each pore type (pore surface area of 50 nm) is indicated in Table 3. It can be observed that the pore volume and the specific surface area of pores with a diameter smaller than 50 nm account for more than 90% of the total, of which the average proportion of the pore volumes is 95.05% and the average proportion of the specific surface areas is 94.83%.

The pore volume and the specific surface area of micropores, mesopores, and macropores are calculated based on the classification standards of the IUPAC (Table 4). Obviously, the mesoporous ($2\,nm < R < 50\,nm$) volume represents the largest proportion in the pore network of the shale samples, with an average value of 91.33%. Macropores ($r > 50$ nm) are the second most abundant type, with an average of 4.95%. Micropores ($r < 2$ nm) are the least abundant, with an average of 3.72%. The pore specific surface area is mainly mesoporous, with an average of 93.81%.

Table 3: Surface area and pore volume values of the analyzed shale samples.

| Sample number | Hole volume ratio (%) | | Specific surface area ratio (%) | |
|---|---|---|---|---|
| | <50 nm | >50 nm | <50 nm | >50 nm |
| L-24 | 0.950445 | 0.049555 | 0.942868 | 0.057132 |
| L-27 | 0.954351 | 0.045649 | 0.942854 | 0.057146 |
| L-29 | 0.948322 | 0.051678 | 0.964788 | 0.057041 |
| L-35 | 0.949041 | 0.050959 | 0.942839 | 0.057161 |

Based on the obtained results, it is clear that the pore volumes of the shale samples are dominated by micropores and mesopores with a small pore radius ($r < 50$ nm). They represent the main space for gas enrichment in the rock. Mesopores and macropores mutually control the pore specific surface area of the samples, and, consequently, there is a significant amount of adsorbed gas in these two types of pores.

*3.5. Controlling Factors of Shale Pore Development.* The development of pores in the shale reservoir is affected by several factors such as the mineral composition and the thermal maturity of the organic matter in the shale rock. Among these, the predominant parameters controlling the shale pore development include the total organic carbon content (TOC), the vitrinite reflectance, the type of organic matter, and the water saturation. Previous studies indicate that organic matter is characterized by the development of numerous micro- and nanopores. Generally, with the increase of organic matter contents and thermal maturity, the pore volume in the rock also increases. Ambrose et al. consider that reservoir rocks are defined by various types of organic matter. Intense microbial action creates micropores and capillaries, which constitute the main pore volume

Table 4: Distribution of the surface area and the pore volume of the shale samples based on IUPAC standards.

| Sample number | Hole volume ratio (%) | | | Specific surface area ratio (%) | | |
|---|---|---|---|---|---|---|
| | <2 nm | 2-50 | >50 nm | <2 nm | 2-50 | >50 nm |
| L-24 | 0.03199 | 0.918454 | 0.049555 | 0.004392 | 0.938476 | 0.057132 |
| L-27 | 0.039148 | 0.915203 | 0.045649 | 0.003931 | 0.938923 | 0.057146 |
| L-29 | 0.040328 | 0.907993 | 0.051678 | 0.007343 | 0.935616 | 0.057041 |
| L-35 | 0.037504 | 0.911537 | 0.050959 | 0.003452 | 0.939387 | 0.057161 |

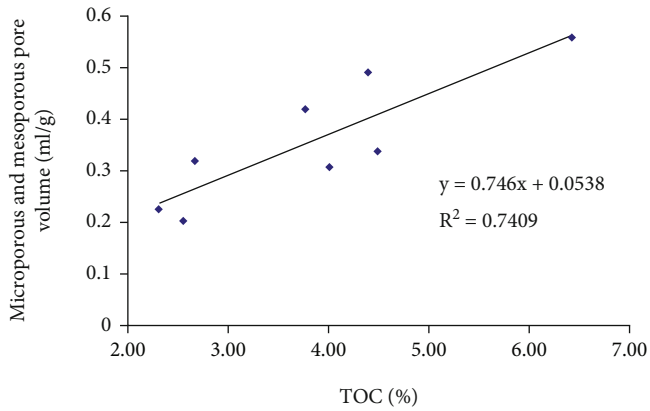


Figure 7: The relationship between the TOC and the microporous and mesoporous pore volumes.

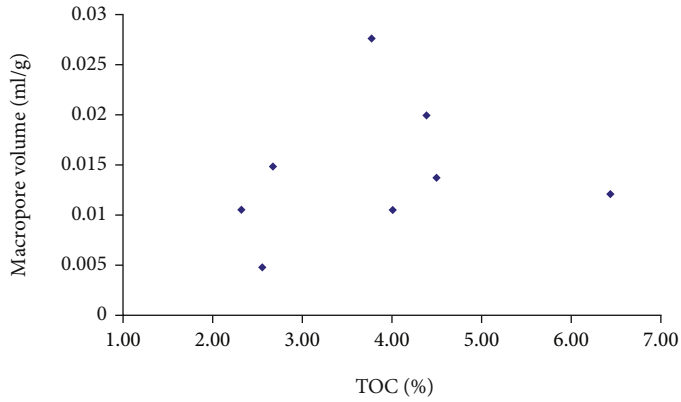


Figure 8: The relationship between the TOC and the macropore volume.

of the rocks. Ross et al. suggest that clay minerals in shale gas reservoirs are characterized by considerable micropore volumes and large pore surface areas.

The correlation between the total organic carbon content (TOC) and the pore volume and the specific surface area of the different pore types is illustrated in Figures 7–10. Total organic carbon content (TOC) has a good correlation with the pore volume, and the specific surface area of micropores and mesopores has a poor correlation with the pore volume and the specific surface area of macropores. With the gradual increase of the total organic carbon, the pore volume and pore specific surface area of micropores and mesopores also increase, which indicates that many micropores and mesopores are predominantly developed in the organic matter component of the shale reservoir. Although the TOC values of some rock samples are high, the matrix pores are not developed due to their low thermal maturity [2].

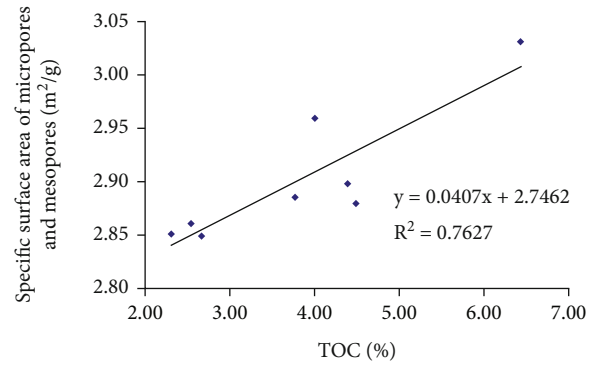


Figure 9: The relationship between the TOC and the specific surface area of micropores and mesopores.

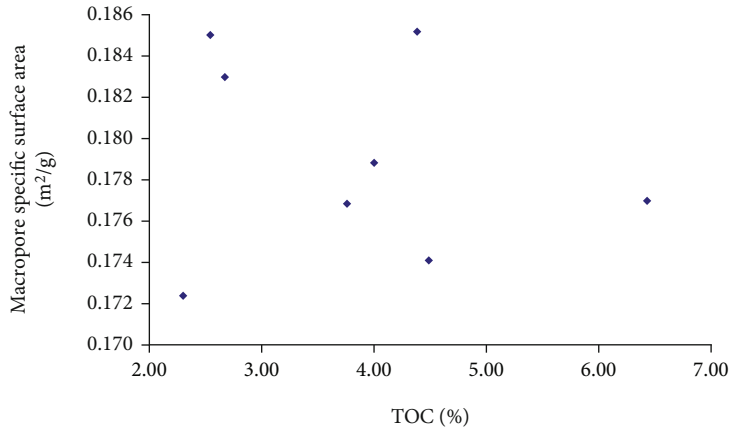


Figure 10: The relationship between the TOC and the macropore specific surface area.

The correlation plots between the clay mineral content and the pore volume and the specific surface area of the different pore types in the shale samples suggest that the clay mineral content has a good correlation with the pore volume and the specific surface area of macropores but has a poor relationship with the pore volume and the specific surface area of micropores and mesopores. With the increase of the clay content in the rock samples, the pore volume and the specific surface area values of macropores also increase, indicating a good positive correlation. Based on the comparative analysis results of the clay minerals and the macropores, it can be concluded that clay minerals have a certain influence on the development of macropores in the shale reservoir rocks.

Behar et al. consider that the type of organic matter affects the development of mesopores and macropores. The predominant group of pores from the Yanchang Formation shales is mesopores with pore sizes varying between 2 and 50 nm. Kang et al. have demonstrated that the presence of numerous micropores in the organic matter component contributes to the creation of more space for the accumulation of hydrocarbons in shale reservoir rocks. Therefore, it can be inferred that the TOC content plays an important role in the development of the shale reservoir porosity in the study area, while the clay mineral content and other factors control the pore volume of different pore sizes. The combination of these factors generates most of the storage space for the accumulation of shale gas.

## 4. Conclusions

(1) The low-temperature nitrogen adsorption method can efficiently determine the characteristics of the micro- and nanopore network in shale reservoir rocks. Mesopores with a pore size distribution varying between 2 and 50 nm are the predominant group of pores in the shale samples from the Yanchang Formation; however, micropores and macropores are also developed. Flat pores occur in rocks that are more susceptible to gas migration

(2) The maximum pore specific surface area and pore volume of the shale reservoir samples are 12.942 $m^2/g$ and 0.35335 mL/g, respectively. The average pore specific surface area and the average pore volume of the analyzed samples are 4.915 $m^2/g$ and 0.23658 mL/g, respectively. Compared to conventional reservoir rocks, the larger pore specific surface area and pore volume values in shale reservoir rocks create more space for the accumulation of hydrocarbons. Specifically, the pore volume of micropores and mesopores with a smaller pore radius ($r < 50$ nm) has the most important contribution, while the mesopores with a pore size distribution in the range of 2-50 nm provide most of the pore specific surface area of the shale

(3) The correlation analyses between the total organic carbon (TOC) content and the clay mineral content, the pore volume, and the specific surface area of the different pore types indicate that the development of micropores and mesopores is related to the presence of organic matter, and the occurrence of macropores is related to clay mineral contents. Specifically, the total organic carbon content (TOC) plays an important role in the development of the rock pore space in the shale reservoir from the Yanchang Formation and is also an essential parameter that provides storage space for the accumulation of shale gas

## Data Availability

All data included in this study are available upon request by contact with the corresponding author.

## Conflicts of Interest

The authors declare no conflict of interest.

## Acknowledgments

We gratefully acknowledge Chongqing Industry Polytechnic College and National Science and Technology Fund Project (2021-CD02) for their financial support.

## References


[1] K. Han, Y. Ju, G. Wang, S. Bao, H. Bu, and B. Neupane, "Shale composition and pore structure variations in the progradation direction: a case study of transitional shales in the Xu-Huai district, Southern North China," *Journal of Natural Gas Science and Engineering*, vol. 36, pp. 1178–1187, 2016.

[2] C. Liu, Y. Wang, X. M. Hu, Y. L. Han, X. P. Zhang, and L. Z. du, "Application of GA-BP neural network optimized by Grey Verhulst model around settlement prediction of foundation pit," *Geofluids*, vol. 2021, 16 pages, 2021.

[3] S. Y. Wang, J. Q. Li, S. F. Lu, P. F. Zhang, J. Zhang, and W. B. Li, "Development characteristics of organic matter pores of marine shale in the southeastern Chongqing, China," *Journal of Earth Sciences and Environment*, vol. 41, pp. 721–733, 2019.

[4] J. Jiyang, X. U. E. Haitao, T. I. A. N. Shansi et al., "Influence of correction of interfacial tension and wetting angle to the pore size distribution of shale by means of high pressure mercury porosity: a case study of Qingshankou Formation in Songliao Basin," *Geoscience*, vol. 32, no. 1, p. 191, 2018.

[5] Y. Li, Y. G. Zhang, L. Zhang, and J. L. Hou, "Characterization on pore structure of tectonic coals based on the method of mercury intrusion, carbon dioxide adsorption and nitrogen adsorption," *Journal of China Coal Society*, vol. 44, no. 4, pp. 1188–1196, 2019.

[6] P. Wang, P. Lv, Z. X. Jiang et al., "Comparison of organic matter pores of marine and continental facies shale in China: based on focused ion beam helium ion microscopy (FIB-HIM)," *Petroleum Geology Experiment*, vol. 5, pp. 739–748, 2018.

[7] C. Liu, L. Du, X. Zhang, Y. Wang, X. Hu, and Y. Han, "A new rock brittleness evaluation method based on the complete stress-strain curve," *Lithosphere*, vol. 2021, article 4029886, 2021.

[8] W. Sun, L. Du, X. Zhang, Y. Wang, X. Hu, and Y. Han, "A new approach to the characterization of shale pore structure," *Lithologic Reserv.*, vol. 29, pp. 125–130, 2017.

[9] P. Zhang, L. U. Shuangfang, L. I. Junqian, X. Haitao, L. I. Wenbiao, and W. Siyuan, "Quantitative characterization of microscopic pore structure for shales using scanning electron microscopy," *Journal of China University of Petroleum*, vol. 42, no. 2, pp. 19–28, 2018.

[10] J. Klaver, G. Desbois, J. L. Urai, and R. Littke, "BIB-SEM study of the pore space morphology in early mature Posidonia Shale from the Hils area, Germany," *International Journal of Coal Geology*, vol. 103, pp. 12–25, 2012.

[11] K. Jiao, S. Yao, C. Liu et al., "The characterization and quantitative analysis of nanopores in unconventional gas reservoirs utilizing FESEM-FIB and image processing: An example from the lower Silurian Longmaxi Shale, upper Yangtze region, China," *International Journal of Coal Geology*, vol. 128, pp. 1–11, 2014.

[12] A. Busch, S. Alles, Y. Gensterblum et al., "Carbon dioxide storage potential of shales," *International Journal of Greenhouse Gas Control*, vol. 2, no. 3, pp. 297–308, 2008.

[13] H. Han, Y. Cao, S. J. Chen et al., "Influence of particle size on gas-adsorption experiments of shales: an example from a Longmaxi Shale sample from the Sichuan Basin, China," *Fuel*, vol. 186, pp. 750–757, 2016.

[14] C. Yang, J. Zhang, S. Han et al., "Compositional controls on pore-size distribution by nitrogen adsorption technique in the Lower Permian Shanxi Shales, Ordos Basin," *Journal of Natural Gas Science and Engineering*, vol. 34, pp. 1369–1381, 2016.

[15] Y. Zapata and A. Sakhaee-Pour, "Modeling adsorption-desorption hysteresis in shales: acyclic pore model," *Fuel*, vol. 181, pp. 557–565, 2016.

[16] C. Keluo, T. Zhang, C. Xiaohui, H. E. Yingjie, and X. Liang, "Model construction of micro-pores in shale: a case study of Silurian Longmaxi formation shale in Dianqianbei area, SW China," *Petroleum Exploration and Development*, vol. 45, no. 3, pp. 412–421, 2018.

[17] R. Heller and M. Zoback, "Adsorption of methane and carbon dioxide on gas shale and pure mineral samples," *Journal Of Unconventional Oil And Gas Resources*, vol. 8, pp. 14–24, 2014.

[18] E. P. Barrett, L. G. Joyner, and P. P. Halenda, "The determination of pore volume and area distributions in porous substances. I. Computations from nitrogen isotherms," *Journal of the American Chemical Society*, vol. 73, no. 1, pp. 373–380, 1951.

[19] S. Brunauer, P. H. Emmett, and E. Teller, "Adsorption of gases in multimolecular layers," *Journal of the American Chemical Society*, vol. 60, no. 2, pp. 309–319, 1938.

[20] I. Langmuir, "Surface area and pore-size by gas sorption operation manual," *Journal of the American Chemical Society*, vol. 40, pp. 1403–1461, 1918.

[21] G. Cao, M. Lin, L. Ji, W. Jiang, and M. Yang, "Characterization of pore structures and gas transport characteristics of Longmaxi shale," *Fuel*, vol. 258, article 116146, 2019.

[22] R. J. Ambrose, R. C. Hartman, M. Diaz-Campos, I. Y. Akkutlu, and C. H. Sondergeld, "New pore-scale considerations for shale gas in place calculations," in *In SPE unconventional gas conference*, Pittsburgh, Pennsylvania, USA, 2010.

[23] D. J. Ross and R. M. Bustin, "Characterizing the shale gas resource potential of Devonian–Mississippian strata in the Western Canada sedimentary basin: application of an integrated formation evaluation," *AAPG Bulletin*, vol. 92, no. 1, pp. 87–125, 2008.

[24] H. Ran, L. Zhiping, L. Fengpeng, and T. Xuan, "Study on the applicability of adsorption models to shale gas," *China Petroleum Exploration*, vol. 23, no. 1, p. 100, 2018.